ELSEVIER

Int. J. Devl Neuroscience 23 (2005) 599–612

INTERNATIONAL JOURNAL of DEVELOPMENTAL NEUROSCIENCE

www.elsevier.com/locate/ijdevneu

Caveolin isoform expression during differentiation of C6 glioma cells

W.I. Silva [a,*], H.M. Maldonado [c], G. Velázquez [a], M. Rubio-Dávila [a], J.D. Miranda [a], E. Aquino [b], N. Mayol [c], A. Cruz-Torres [a], J. Jardón [a], I.K. Salgado-Villanueva [a]

[a] *Department of Physiology, School of Medicine, University of Puerto Rico, Medical Sciences Campus, P.O. Box 365067, San Juan, PR 00936-5067, USA*

[b] *Department of Microbiology, School of Medicine, University of Puerto Rico, Medical Sciences Campus, P.O. Box 365067, San Juan, PR 00936-5067, USA*

[c] *Department of Pharmacology, School of Medicine, Universidad Central del Caribe, School of Medicine, Bayamón, PR, USA*

Received 26 May 2005; received in revised form 18 July 2005; accepted 19 July 2005

Abstract

Caveolae, a specialized form of lipid rafts, are cholesterol- and sphingolipid-rich membrane microdomains implicated in potocytosis, endocytosis, transcytosis, and as platforms for signal transduction. One of the major constituents of caveolae are three highly homologous caveolin isoforms (caveolin-1, caveolin-2, and caveolin-3). The present study expands the analysis of caveolin isoform expression in C6 glioma cells. Three complementary approaches were used to assess their differential expression during the dibutyryl-cyclic AMP-induced differentiation of C6 cells into an astrocyte-like phenotype. Immunoblotting, conventional RT-PCR, and real-time RT-PCR analysis established the expression of the caveolin-3 isoform in C6 cells, in addition to caveolin-1 and caveolin-2. Similar to the other isoforms, caveolin-3 was associated with light-density, detergent-insoluble caveolae membrane fractions obtained using sucrose-density gradient centrifugation. The three caveolin isoforms display different temporal patterns of mRNA/protein expression during the differentiation of C6 cells. Western blot and real-time RT-PCR analysis demonstrate that caveolin-1 and caveolin-2 are up-regulated during the late stages of the differentiation of C6 cells. Meanwhile, caveolin-3 is gradually down-regulated during the differentiation process. Indirect immunofluorescence analysis via laser-scanning confocal microscopy reveals that the three caveolin isoforms display similar subcellular distribution patterns. In addition, co-localization of caveolin-1/caveolin-2 and caveolin-1/caveolin-3 was detected in both C6 glioma phenotypes. The findings reveal a differential temporal pattern of caveolin gene expression during phenotypic differentiation of C6 glioma cells, with potential implications to developmental and degenerative events in the brain.

Keywords: C6 glial cells; Caveolae; Caveolin; Plasmalemmal vesicles

Abbreviations: AD, Alzheimer's disease; BSA, bovine serum albumin; CAV, caveolae; cav1, caveolin-1; cav2, caveolin-2; cav3, caveolin-3; DTT, 1,4-dithiothreithol; db-cAMP, dibutyryl cyclic AMP; EDTA, ethylenediaminetetraacetic acid; GFAP, glial fibrillary acidic protein; HEPES, *N*-[2-hydroxyethyl]-piperazine-*N*-[2-ethane sulfonic acid]; IgG, immunoglobulin G; MES, 2-morpholinethanesulfonic acid; MeOH, methanol; MBS, Mes-buffered saline; mAb, monoclonal antibody; Na_2CO_3, sodium carbonate; NH_4Cl, ammonium chloride; pAb, polyclonal antibody; PBS, phosphate-buffered saline; PVDF, polyvinylidine difluoride; PMSF, phenyl-methyl-sulfonyl-fluoride; SC, Schwann cells; Tris–HCl, tris(hydroxymethyl) aminomethane hydrochloride

* Corresponding author. Tel.: +1 787 751 2042; fax: +1 787 281 8372.
E-mail address: wsilva@rcm.upr.edu (W.I. Silva).

0736-5748/$30.00 © 2005 ISDN. Published by Elsevier Ltd. All rights reserved.
doi:10.1016/j.ijdevneu.2005.07.007

1. Introduction

Originally referred to as plasmalemmal vesicles, caveolae (CAV) are typically defined as flask-shaped, non-clathrin-coated invaginations of the plasma membrane (Bruns and Palade, 1968a,b; Palade, 1961). Based on their chemical composition (sphingolipid- and cholesterol-rich) and biophysical properties (resistance to solubilization at low temperatures by non-ionic detergents and light buoyant density), CAV have been referred to as specialized lipid rafts (Helms and Zurzolo, 2004; Simons and Toomre, 2000). These specialized CAV membrane microdomains have proven and emerging physiological and pathophysiological roles (Cohen et al., 2004; Engelman et al., 1998; Hnasko and Lisanti, 2003; Nichols, 2003; Quest et al., 2004; Razani and Lisanti, 2001; Razani et al., 2001; Shatz and Liscovitch, 2004). In this context, CAV plays a role in clathrin-independent endocytosis and transcytosis (Conner and Schmid, 2003; Nichols, 2003), potocytosis (Mineo and Anderson, 2001), signal transduction (Chini and Parenti, 2004; Cohen et al., 2004; Okamoto et al., 1998), internalization of specific-pathogens and toxins (Lakadamyali et al., 2004; Nichols, 2003; Pietiainen et al., 2004; Rohde et al., 2003), tumor suppression (Lisanti et al., 1995a,b; Razani et al., 2000, 2001), certain forms of muscular dystrophy (Bushby, 1999; Galbiati et al., 2001; Nishino and Ozawa, 2002; Razani et al., 2000; Woodman et al., 2004), diabetes (Cohen et al., 2003), vascular diseases (Everson and Smart, 2001; Frank et al., 2003), and Alzheimer's disease (AD) (Gaudreault et al., 2004; Hashimoto and Masliah, 2003; Nishiyama et al., 1999).

The physiological importance of CAV is intimately linked to the functional capabilities of their main constituent or signature proteins, the caveolins. Studies on the molecular composition of CAV-identified caveolin, a 21 kDa membrane protein originally described as a primary v-src tyrosine kinase substrate (Glenney, 1992), as a principal constituent of CAV (Glenney and Soppet, 1992; Rothberg et al., 1992). Caveolin 1 (cav1) is the first member of a multigene family, which includes at least two cav1 isoforms (alpha and beta, 24 and 21 kDa, respectively): caveolin-2 (cav2, 20 kDa) and caveolin-3 (cav3, 18 kDa) (Williams and Lisanti, 2004). Still though, apparent higher molecular weight species, probably due to their oligomerization and protein-interaction properties, have been reported in tissues like brain (Ikezu et al., 1998). Although CAV/caveolins are present in most cells, they are most abundant in terminally differentiated cell types: endothelia, adipocytes, muscle cells, and type I pneumocytes. In contrast, CAV/caveolins are reduced or absent in fibroblasts transformed by certain activated oncogenes (Koleske et al., 1995). Furthermore, morphologically identifiable CAV are absent from cav1 and cav3 knock-out mice model systems, supporting the role of caveolins in the biogenesis of CAV (Cohen et al., 2004; Hnasko and Lisanti, 2003; Quest et al., 2004; Razani and Lisanti, 2001). Since caveolin's original characterization, the detection of caveolins in the brain had been elusive, but a series of experimental evidence has clearly established that brain tissue expresses the three caveolin isoforms (Cameron et al., 1997; Henke et al., 1996; Ikezu et al., 1998). This has led to an increased interest and attention to elucidate the role(s) and function(s) of CAV/caveolins in the nervous system.

In the case of glia, valuable studies conducted on primary cell cultures and established glial cell lines have also demonstrated the expression of the caveolin isoforms, particularly cav1 and cav2 (Bushby, 1999; Cameron et al., 2002; Colasanti et al., 1998; Mikol et al., 1999; Silva et al., 1999). The caveolins in glia are linked to an active subcellular transport machinery (Megias et al., 2000), and relate to the original morphological studies that identified plasmalemmal vesicles in peripheral Schwann cells (Mugnaini et al., 1977), fibrous astrocytes from cat optic nerve (Massa, 1982), and mixed cultures of rat fetal glial cells (Massa and Mugnaini, 1985). An important role for the glial compartment in the regulation of drug transport in the nervous system has been suggested due to the cellular/subcellular location and functional expression of P-glycoprotein, an ATP-dependent membrane-associated efflux transporter, in CAV from rat astrocytes (Demeule et al., 2000; Ronaldson et al., 2004). Additional studies support the well-established roles of CAV/caveolins in signal transduction (Abulrob et al., 2004; Arvanitis et al., 2004; Colasanti et al., 1998; Ge and Pachter, 2004; Mentlein et al., 2001; Teixeira et al., 1999) and cholesterol homeostasis (Ito et al., 2002, 2004).

Despite these advances in our knowledge of glial cell CAV/caveolins, analysis of the regulation of caveolin expression in these cells has been very limited to date. In the peripheral nervous system (PNS), Schwann cells (SC) (as well as a series of SC cell lines) express cav1, and its levels are down-regulated after axotomy (Mikol et al., 1999). Meanwhile, a recent study by Zschoecke et al. (2005) reports region-specific down-regulation of cav1 and cav2 expression in the brain during the differentiation of primary cell cultures of astrocytes. In contrast, in brain tissue sections from authentic AD patients and an established transgenic mouse model of AD, there is a dramatic up-regulation of caveolin-3 immunoreactivity in astroglial cells surrounding senile plaques (Nishiyama et al., 1999). Despite the evidence for the expression of the cav3 isoform in oligodendrocytes and astrocytes, and its relevance to the pathophysiology of Alzheimer's disease (Nishiyama et al., 1999), no other study on glial cells to date has reported changes in its pattern of expression. Along this line, the present study furthers our analysis and understanding of caveolin mRNA and protein expression in C6 glioma cells. The study demonstrates that C6 cells also express the cav3 isoform and provides evidence for differential patterns of caveolin expression during the experimentally induced differentiation of C6 into an astrocyte-like phenotype, including a prominent down-regulation of the cav3 isoform, parallel to an up-regulation of cav1 and cav2.

2. Materials and methods

2.1. Materials

Cell culture, immunoblotting, and cellular fractionation reagents were obtained from Sigma Chemical Co. (St. Louis, MO): ethylene-diamine-tetraacetic acid (EDTA), nutrient mixture F-10 Ham media, antibiotic/antimycotic solution; HEPES buffer, 1,4-dithiothreithol (DTT), magnesium chloride ($MgCl_2$), phenyl-methyl-sulfonyl-fluoride (PMSF), leupeptin, antipain, bestatin, chymostatin, pestatin A, Sigmacote, Triton X-100, sucrose, bovine serum albumin (BSA), MES buffer, sodium chloride (NaCl), and urea. Fetal bovine serum (FBS), Hank's balance salt solution (HBSS), phosphate-buffered saline (PBS), and trypsin were obtained from Invitrogen Life Technologies (Carlsbad, CA). Electrophoresis reagents were purchased from Bio-Rad Laboratories (Hercules, CA): Coomasie blue, Laemmli sample buffer, β-mercaptoethanol, methanol, Precision Plus Protein™ Standards, sodium dodecyl sulfate (SDS), 10× Tris/glycine/SDS buffer, Tris–HCl buffer (0.5 M, pH 6.8 and 1.5 M, pH 8.8), and PVDF membranes.

The following antibodies were obtained from BD Biosciences (Lexington, KY): the rabbit anti-caveolin-1 (affinity-purified pAb; directed against caveolin-1 residues 1–97) and the mouse anti-caveolin-1 (mAB, clone 2297); the mouse anti-caveolin-2 (mAb, directed against the extreme C-terminus of caveolin-2; clone 65), the mouse anti-caveolin-3 (mAB, directed against the extreme N-terminus of caveolin-3; clone 26) and the mouse anti-GFAP monoclonal antibody mix (cocktail of mAb clones). Alexa-coupled secondary antibodies were from Molecular Probes (Eugene, OR).

2.2. Cell cultures

Rat C6 glioma cells (Benda et al., 1968; Pfeiffer et al., 1970) (Cell Systems, Seattle, WA) were routinely propagated as confluent monolayers grown in tissue culture flasks (T_{75}). C6 glioma cells were grown in nutrient mixture Ham's F-10 media containing 1% antibiotic/antimycotic and 10% FBS. Medium removal was done every other day. Cell passage was done weekly. For immunofluorescence analysis, C6 glioma cells were seeded on coverslips of dual-chamber slides at a density of 1×10^4 cells/well and incubated at 37 °C, under an atmosphere of 5% CO_2. Subconfluent monolayer cells were used for experiments at 2 days after passage. Induction of differentiation into astrocyte-like cells was achieved by the addition of 1 mM dibutyryl cyclic AMP (db-cAMP) and reduction of growth media to 1% FBS.

2.3. Cellular fractionation

Preparation of total homogenates and equilibrium density gradient isolation of caveolin-enriched membrane fractions were done as described previously (Lisanti et al., 1995a,b; Sargiacomo et al., 1993; Silva et al., 1999). Briefly, all cellular fractionation procedures were performed at 4 °C. For the preparation of total homogenates, the medium was removed from the confluent monolayers of C6 glioma and the cells washed with PBS. After addition of trypsin, cells were centrifuged and the pellet resuspended and homogenized in lysis buffer (20 mM HEPES, 2 mM DTT, 10 mM $MgCl_2$, 0.1 mg/ml BSA at pH 7.0), plus a cocktail of protease inhibitors (100 μg/ml each of leupeptin, antipain, bestatin, chymostatin, and pepstatin A). Protein concentration was determined using the Bradford assay and samples diluted either in Laemmli sample buffer solution, or urea sample buffer (4% SDS, 8 M urea, 62 mM EDTA, 0.2% mercaptoethanol, and 0.015% bromophenol blue). The latter sample buffer modification improves detection of the cav3 isoform.

To generate the detergent-insoluble density gradient fractions, C6 glioma cells were processed as previously described (Silva et al., 1999). Briefly, rat C6 glioma cells were rinsed twice with MBS (25 mM MES and 15 M NaCl). Then, MBS containing 2% Triton X-100 and 1 mM PMSF was added and the cells scraped and homogenized. The resulting homogenate was separated over a discontinuous sucrose-density gradient, prepared by adjusting the homogenate to 40% sucrose by addition of 80% sucrose in MBS, and overlaying with 4 ml of 30% sucrose in MBS, and 4 ml 5% sucrose in MBS. The sample was centrifuged at 39,000 rpm for 22 h in a SW 41 rotor (Beckman Instruments). Twelve 1 ml fractions were collected from the top of the gradient, diluted three-fold with MBS, and centrifuged at 100,000 × g for 30 min at 4 °C. The resulting pellets were resuspended in MBS and stored at −80 °C, or alternatively directly resuspended in SDS-PAGE sample buffer.

2.4. SDS-PAGE and immunoblotting

SDS-PAGE and immunoblot analysis of the pellets and gradient fractions was done as previously described (Silva et al., 1999). In brief, equal total homogenate amounts (∼10 μg protein) or volumes (gradient fractions), plus the molecular weight standards, were resuspended in the sample buffers described above, and separated in 10–15% SDS polyacrylamide gels (Bio-Rad Laboratories, Hercules, CA). After electrophoresis, the gel was transferred overnight to a PVDF membrane using a mini trans-blot apparatus (Bio-Rad Laboratories, Hercules, CA) at 4 °C. PVDF membranes were stained with India ink to verify transfer efficiency and to quantitate total protein content using a Bio-Rad Gel Doc 1000 system (Bio-Rad Laboratories, Hercules, CA). Subsequently, membranes were incubated overnight (at 4 °C) with a primary polyclonal antibody against cav1 (1:10,000 dilution), and monoclonal antibodies against cav2 (1:5000 dilution) and cav3 (1:2000 dilution). After addition of the corresponding secondary antibodies, membranes were

processed using the enhanced chemiluminescence assay (SuperSignal® West dura extended duration substrate; Pierce, Rockford, IL) as described by the manufacturer.

2.5. Immunofluorescence

Sample preparation for immunofluorescence and laser-scanning confocal microscopy (LSCM) was done as previously described (Silva et al., 1999). In brief, media was decanted and the cells rinsed in PBS. Cells were fixed with 100% methanol (−20 °C), rinsed, and treated with 100 mM NH_4Cl in PBS. After rinsing, cells were permeabilized with 0.1% Triton X-100 and subsequently incubated in 2% BSA in PBS. The slides were incubated with primary antibodies (1:150 for anti-cav1; 1:50 for anti-cav2 and anti-cav3) for 1 h at room temperature. After rinsing, slides were incubated with the secondary antibodies (1:300 for anti-rabbit-Alexa 488, anti-mouse IgG-Alexa 488, or -Alexa 633) for 1 h at room temperature. The slides were washed and mounted with antifading medium (Slowfade® antifade kit, Molecular Probes, Eugene, OR). Indirect immunofluorescence and co-localization studies were done using a Nikon Confocal Imaging System (TE2000 Inverted Microscope and C1 Eclipse Confocal Setup; Nikon Instruments Inc., Melville, NY).

2.6. Reverse transcriptase-PCR analysis

2.6.1. Quantification of caveolin isoform mRNA expression

To initiate the determination of the relative expression of the mRNA of the caveolin isoforms, we took two complementary approaches: semi-quantitative conventional RT-PCR and real-time RT-PCR analysis. Total RNA was isolated from glioma cells using trizol reagent (Invitrogen Life Technologies, Carlsbad, CA) according to the manufacturer's instructions. To remove possible genomic contamination, the extracted RNA was treated with DNAse using the Ambion DNA-free kit (Ambion Inc., Austin, TX). Integrity of the extracted total RNA was electrophoretically verified by ethidium bromide staining and observed in a denaturant agarose gel.

2.6.2. Reverse transcriptase-polymerase chain reaction (RT-PCR)

Reverse transcription reaction was performed using ~1.5 μg total RNA. First strand cDNA was synthesized using the Superscript™ II RNAse H^- reverse transcriptase kit (Invitrogen Life Technologies) with Oligo-dT as the primer following manufacturer's instructions. To assay for possible genomic DNA contamination of the RNA sample, a mock cDNA reaction, which included all reagents except reverse transcriptase, was prepared for each RNA extraction. This mock cDNA was subsequently used in a PCR reaction. The following PCR primers were used for the detection of cav1, cav2, cav3, and GAPDH transcripts: cav1 sense primer 5′-*AGCATGTCTGGGGGTAAATACG*-3′ and antisense primer 5′-*CCTCCATCCCTGAAATGTCCT*-3′ (560 bp); cav2 sense primer 5′-*GCTCAACTCGCATCTCAAGCT*-3′ and antisense primer 5′-*TCTGTCACACTCTTCCATATT*-3′ (260 bp); cav3 sense primer 5′-*CCAAGAACATCAATGAGGACATTGTG*-3′ and antisense primer 5′-*TCGCAGCACCACCTTAATGTT-GCT*-3′ (358 bp); and GAPDH sense primer 5′-*ACCA-CAGTCCATGCCATCAC*-3′ and antisense 5′-*TCCACCA-CCCTGTTGCTGTA*-3′ (452 bp). PCR reactions were run at 94 °C for 1 min (denaturation), 1.5 min for annealing at 60 °C (cav1, cav3, and GAPDH) and 50 °C (cav2), and 72 °C for 1.5 min for extension. After an initial 3 min hot start, PCR reactions were done between 29 and 33 cycles and ended with a final extension at 72 °C for 5 min. PCR products were subsequently analyzed by electrophoresis on a 1% agarose gel impregnated with ethidium bromide (0.5 μg/ml). Densitometric analysis was performed using the Bio-Rad Laboratories Gel Doc 1000 and its Molecular Analysis Software (Hercules, CA). This procedure allowed confirmation of the expression of the mRNA for the caveolin isoforms in C6 glioma cells.

2.7. Real-time reverse transcription PCR

Validation of temporal caveolin isoform mRNA expression was performed with real-time RT-PCR analysis. For this procedure, first strand cDNA was synthesized using the iScript™ cDNA synthesis kit (Bio-Rad). Gene analysis involved standard desalting primers designed with Beacon Designer 3 (Premier Biosoft International, Palo Alto, CA) for cav1, cav2, and cav3 genes (IDT® Integrated DNA Technologies Inc., Coralville, IA). The following PCR primers were used for the detection of cav1, cav2, cav3, GFAP, and GAPDH transcripts: cav1 sense primer 5′-*CGTAGACTCCGAGGGACATC*-3′ and antisense primer 5′-*CGTACACTTGCTTCTCATTCAC*-3′ (110 bp); cav2 sense primer 5′-*GCTGGGCTTCGAGGATGTG*-3′ and antisense primer 5′-*AGGAACACCGTCAGGAACTTG*-3′ (126 bp); cav3 sense primer 5′-*CCAAGAACATCAATGAGGA-CATTGTG*-3′ and antisense primer 5′-*GTGGCAGAAGGA-GATACAG*-3′ (211 bp); GFAP sense primer 5′-*AAGAGACAGAGGAGTGGTATCG*-3′ and antisense primer 5′-*AGTCGTTAGCTTCGTGTTTGG*-3′ (102 bp) and GAPDH sense primer 5′-*AACTTTGGCATCGTGGAA*-3′ and antisense primer 5′-*TACATTGGGGGTAGGAACAC*-3′ (222 bp). Real-time RT-PCR was performed in an iCycler (Bio-Rad Laboratories) using the iQ™ SYBR® Green Supermix (Bio-Rad Laboratories) as a fluorescence dye for the presence of double-stranded DNA. After optimization of PCR conditions, reactions with SYBR® Green PCR master mix, 10 μM forward/reverse primer and 100 ng cDNA were prepared. PCR parameters were 95 °C for 3 min (required for iTaq™ DNA polymerase activation), 40 cycles of 95 °C for 10 s and 1 min annealing at 50 °C (cav1 and cav2), 55 °C (GAPDH), 55.4 °C (GFAP), and 61.3 °C (cav3). The generation of specific PCR products was confirmed by

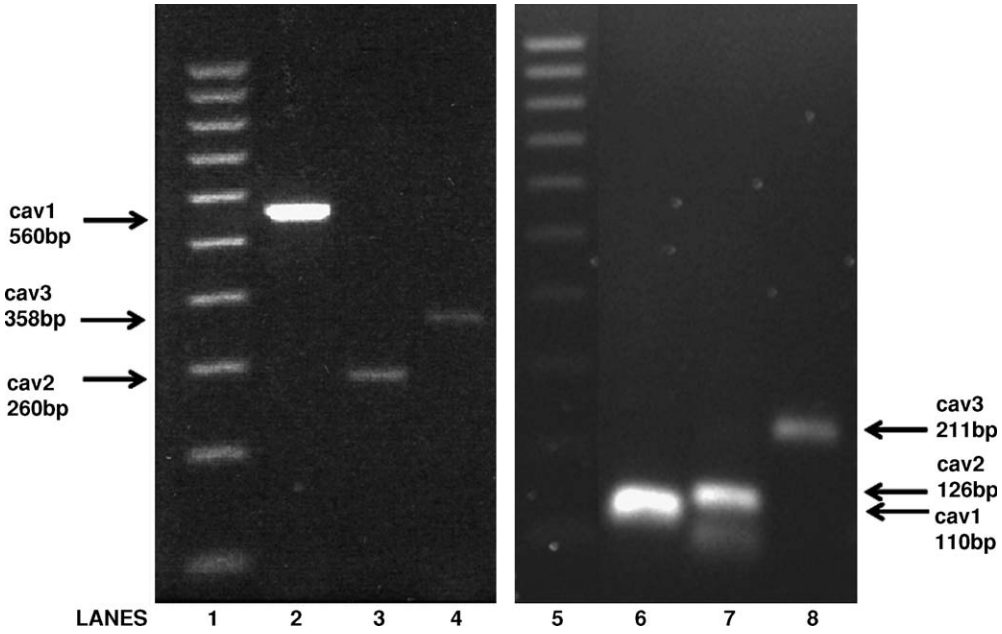

Fig. 1. RT-PCR analysis of cav1, cav2, and cav3 in C6 glioma cells. RT-PCR was performed with total RNA obtained from undifferentiated C6 glioma cells using specific primers for cav1, cav2, and cav3 (see Section 2). Reaction products obtained from conventional RT-PCR (lanes 2–4) and real-time RT-PCR (lanes 6–8) were separated using a 2% agarose gel containing ethidium bromide. The DNA ladder corresponds to the first and fifth lanes and the expected sizes of the reaction products for the three caveolin isoforms are indicated on the left and right sides of the figure.

melting curve analysis, and separation of the products over agarose gels (see Fig. 1). Optimization of the real-time PCR efficiencies for the different caveolin isoforms was calculated from the given slopes using the iCycler Software. PCR cycle number that generated the first fluorescence signal above threshold (threshold cycle, C_T) was determined and subsequently a comparative C_T method was used to measure relative gene expression. The X factor by which the amount of caveolin isoform (or GFAP) has changed in control (T_0) and differentiating cells (T_8, T_{24}, and T_{48}) using GAPDH for normalization was calculated with the following formula (Livak and Schmittgen, 2001):

$$X = 2^{-\Delta\Delta C_T}, \text{ where } \Delta\Delta C_T = [(C_{T(\text{cavs})} - C_{T(\text{GAPDH})})]_{\text{time}(X\,\text{h})} - [(C_{T(\text{cavs})} - C_{T(\text{GAPDH})})]_{\text{control}}$$

2.8. Statistical analysis

Mean values of data from at least four independent experiments were subsequently calculated and plotted as a percentage compared with untreated controls (which were set to 100%). Standard errors were calculated by one-way analysis of variance (ANOVA) and by Students's paired t-test using Graph Pad Prism software (Graph Pad Software Inc., San Diego, CA). Significance between groups was further analyzed using the post hoc Tukey's test.

3. Results

3.1. RT-PCR analysis demonstrates that C6 glioma cells express the messenger RNA for the three caveolin isoforms

In a previous study (Silva et al., 1999), the expression of cav1 and cav2 in C6 glioma cells was established using immunoblot analysis of total C6 cell homogenates, density gradient sedimentation, and indirect immunofluorescence. In the present study, the analysis of caveolin isoform expression was expanded to the mRNA and proteins levels. Conventional RT-PCR and real-time RT-PCR analytical approaches were applied to determine the presence of the mRNA for the three caveolin isoforms in C6 astroglia is shown in Fig. 1. Using specific primers for the different caveolin isoforms reveals, with either RT-PCR approach, the expression of the mRNA for the three caveolin isoforms. Using conventional RT-PCR analysis the reaction yielded the expected product sizes for each of the caveolin isoforms: cav1 (560 bp), cav2 (260 bp), and cav3 (358 bp) (Fig. 1, lanes 2–4). Real-time RT-PCR analysis further corroborated the expression of the message for the three caveolin isoforms. Melt curves using a different set of specific primers for each of the caveolin isoforms revealed the expression of a single reaction product (data not shown), which when separated using agarose gel electrophoresis revealed, as well, reaction products of the corresponding expected sizes (Fig. 1, lanes 6–8): cav1 (110 bp), cav2 (126 bp), and cav3 (211 bp). These findings further

substantiate the expression of the message for the cav1 isoform in C6 cells, while providing evidence for the first time of the expression of the mRNA for the cav2 and cav3 isoforms.

3.2. Immunoblot analysis of total homogenates and density-gradient-derived caveolin-enriched membrane fractions further demonstrates that C6 glioma cells express the caveolin-3 isoform

To further provide evidence on the expression of the cav3 isoform in C6 astroglioma cells, total cell homogenates were prepared and resuspended in a modified SDS-PAGE sample buffer, which included urea and 4% SDS (see Section 2). Under these conditions, Western blot analysis reveals cav3 immunoreactivity of ~18 kDa (Fig. 2, panel A). In order to determine that the cav3 immunoreactivity displays buoyant density and detergent-insolubility properties typical of the caveolins, C6 glioma cells were solubilized in Triton X-100 and detergent lysates fractionated by equilibrium centrifugation on 5–40% discontinuous sucrose-density gradients.

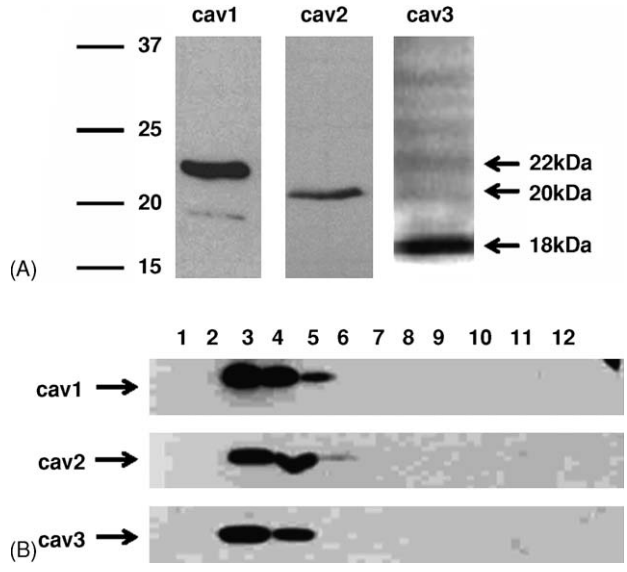

Fig. 2. Immunoblot analysis of the expression of cav1, cav2, and cav3 in total homogenate (panel A) and density-gradient (panel B) fractions of C6 glioma cells. (Panel A) Immunoblot analysis of the different caveolin isoforms (indicated at the top of panel A) was performed in total homogenate fractions from undifferentiated C6 glioma cells. Equal amounts of sample (~10 μg protein) were loaded and then separated by SDS-PAGE. The relative protein content was verified by means of India ink. Bars on the left side indicate the migration of molecular weight standards. The molecular weights for the different caveolin isoforms are indicated on the right side of the figure: cav1 (~22 kDa), cav2 (~20 kDa), and cav3 (~18 kDa). (Panel B) Isolation of cav1-, cav2-, and cav3-enriched membrane fractions from C6 glioma cells using a Triton X-100-based method. Equal volumes of fractions collected across the gradients were resolved by SDS-PAGE and immunoblots done using the indicated anti-caveolin antibodies. All isoforms co-fractionate with the characteristic light-density, triton-insoluble membrane fractions (3–5). Fraction number is indicated horizontally (numbers indicated above the figure—fraction 1: top and fraction 12: bottom).

Fig. 2 (panel B) demonstrates that, consistent with the known properties of CAV, light-density, Triton X-100-insoluble membrane fractions enriched in cav1, cav2, and cav3 were obtained as revealed by the peak of immunoreactivity in the light-density fractions 3–5 near the 5–30% sucrose interphase.

3.3. Indirect immunofluorescence analysis of cav3 in undifferentiated C6 glioma cells

The expression of caveolin has been shown to correlate with the presence of morphologically identifiable CAV. As previously shown (Silva et al., 1999), the cav1 and cav2 immunoreactive species of C6 glioma cells seen in Western blots were ascribed to CAV or CAV-like membrane domains as determined by indirect immunofluorescence analysis. A similar approach was undertaken for the cav3 of C6 glioma cells (Fig. 3). Taking advantage of laser-scanning confocal microscopy (LSCM), the co-localization of the three caveolin isoforms was evaluated in C6 cells, as well. As had been previously established cav1 and cav2 display patterns of subcellular distribution characterized by intensely fluorescent puncta throughout the cytoplasm and diffuse micropatches at the level of the plasmalemma. Perinuclear staining was also detected, consistent with caveolin's localization in the *trans* Golgi region. Fig. 3 also demonstrates that plasmalemma micropatches, consistent with CAV, display significant co-localization of both cav1 and cav2. A similar subcellular distribution pattern was revealed for cav3, both in terms of its subcellular pattern of distribution (plasmalemma caveolar micropatches and perinuclear staining), and in terms of its co-localization with cav1 and cav3 (Fig. 3).

3.4. Caveolin isoform message expression during differentiation of C6 glioma cells determined via real-time RT-PCR

The value of cultured C6 astroglial cells, as a model system for the study of the role of CAV and the caveolin isoforms in glial cell neurobiology, is further expanded due to the established conditions to experimentally induce the in vitro differentiation of C6 glioma cells into an astrocyte-like phenotype. The ability to induce the differentiation of C6 cells into an astrocyte-like phenotype was validated by determining the expression of the message for GFAP using real-time RT-PCR (Fig. 4, panel B) and via Western blots (Fig. 5). Under these experimental conditions, the expected up-regulation of the GFAP message and protein is observed, being particularly prominent and significant at 48 h (T_{48}). The expression of the message for the three caveolin isoforms was determined via standardized, conventional RT-PCR at different time points after induction of differentiation with db-cAMP (time points (h): 0, 8, 24, and 48) (Fig. 4, panel A). The results suggested an up-regulation of cav1 and cav2 during C6 differentiation, parallel to down-regulation of the cav3 isoform messages. During this time course, the

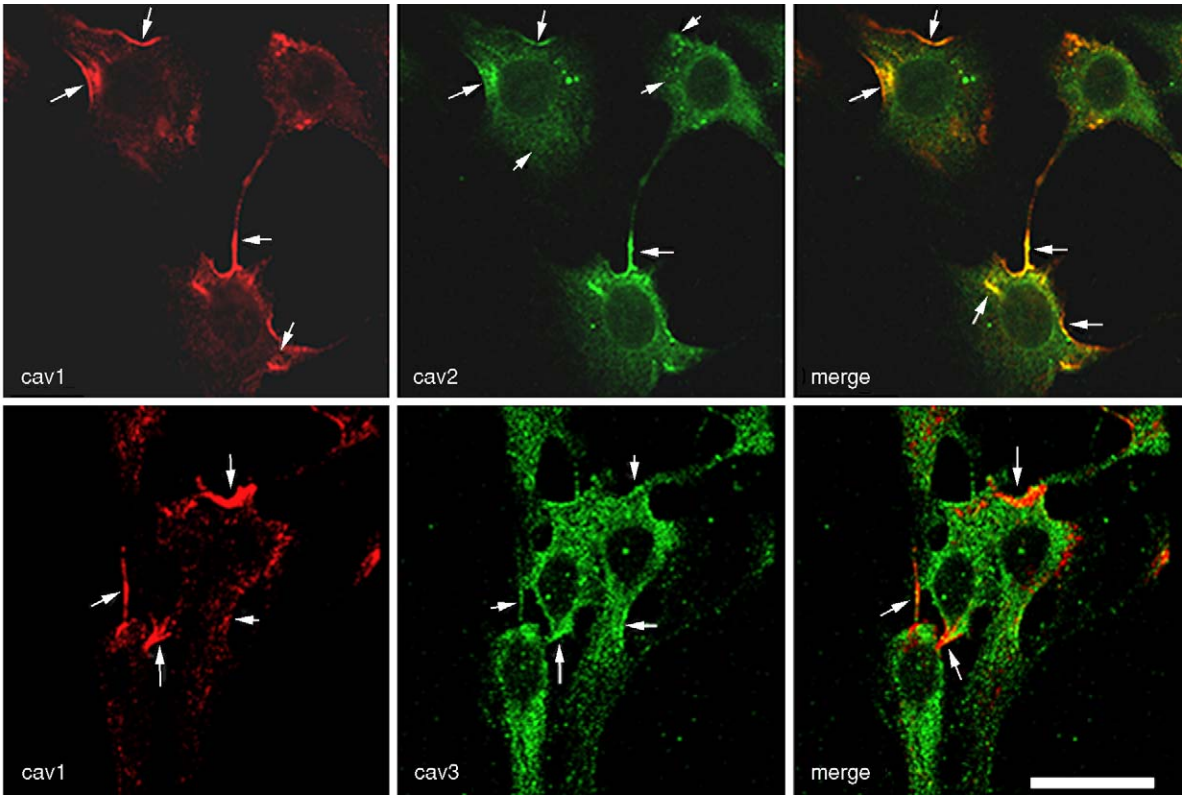

Fig. 3. Analysis of the expression and co-localization of the caveolin isoforms in undifferentiated C6 glioma cells using laser-scanning confocal microscopy. The left column images correspond to immunolabeling using a cav1 primary antibody and an Alexa 633-coupled secondary antibody (red). The middle column images correspond to immunolabeling of cav2 (top) or cav3 (bottom) with Alexa 488-coupled secondary antibodies (green). The last column corresponds to the merge of the cav1/cav2 and cav1/cav3 immunofluorescence signals to determine their co-localization in ''oligodendrocyte-like'' undifferentiated glial cells. The three isoforms display patterns of subcellular distribution typical of caveolins, characterized by intensely fluorescent puncta throughout the cytoplasm (arrow heads) and plasmalemma caveolar micropatches (arrows). Perinuclear staining was also detected, consistent with caveolin's localization in the *trans* Golgi region. On the merged images (right column), co-localization of cav1/cav2 and cav1/cav3 is indicated by the yellow fluorescence signal (arrows). Scale bar: 10 μm. ''For interpretation of the references to color in this figure legend, the reader is referred to the web version of the article.''

relative levels of GAPDH were not statistically significant from those of the T_0 control (Fig. 4, panel A). To obtain a quantitative estimate of caveolin isoform mRNA expression, we utilized real-time RT-PCR (Fig. 4, panel B). This analysis revealed a differential temporal pattern of caveolin mRNA expression during differentiation of C6 glioma cells. The results yield a concomitant up-regulation of cav1 (∼134.1% (±38.3)) and cav2 (∼117.2% (±38.5)), the increased levels being particularly significant for cav1 at T_{48} ($p < 0.01$) and at T_{48} ($p < 0.05$) for cav2 (Fig. 4, panel B). In contrast, there is a gradual and statistically significant ($p < 0.001$) decrease in the levels of the cav3 message at all the time points analyzed, with a maximum decline in its expression to ∼14.1% (±4.6), when compared to the T_0 control group.

3.5. Immunoblot analysis of caveolin isoform expression during differentiation of C6 glioma cells

Immunoblots for the three caveolin isoforms were obtained to determine the relative changes in isoform protein expression during the differentiation of C6 astroglioma cells; cav1, cav2, and the astrocyte marker GFAP protein levels are up-regulated, while cav3 expression is down-regulated after 48 h of induction of differentiation by db-cAMP (Fig. 5). As shown in Fig. 5, under these experimental conditions, the expected up-regulation of GFAP is observed (∼515.42% (±189.61)), being particularly prominent and significant at 48 h ($p < 0.05$). Similar to the patterns of caveolin isoform message expression (Fig. 4), immunoblot analysis of the three caveolin isoforms (Fig. 5, panel A) reveals a differential temporal pattern of caveolin expression. There is a significant up-regulation of cav1 (∼29.73% (±10.7)) and cav2 (∼82.12% (±31.7)) at T_{48} for cav1 ($p < 0.05$) and at T_{48} for cav2 ($p < 0.05$ by *t*-test analysis) (Fig. 5, panel B). In contrast, there is a gradual and statistically significant decrease in the levels of the cav3 protein at the T_{24} ($p < 0.05$) and T_{48} ($p < 0.01$) time points, with a maximum decline in its expression to ∼63.5% (±5.5) when compared to the T_0 control group.

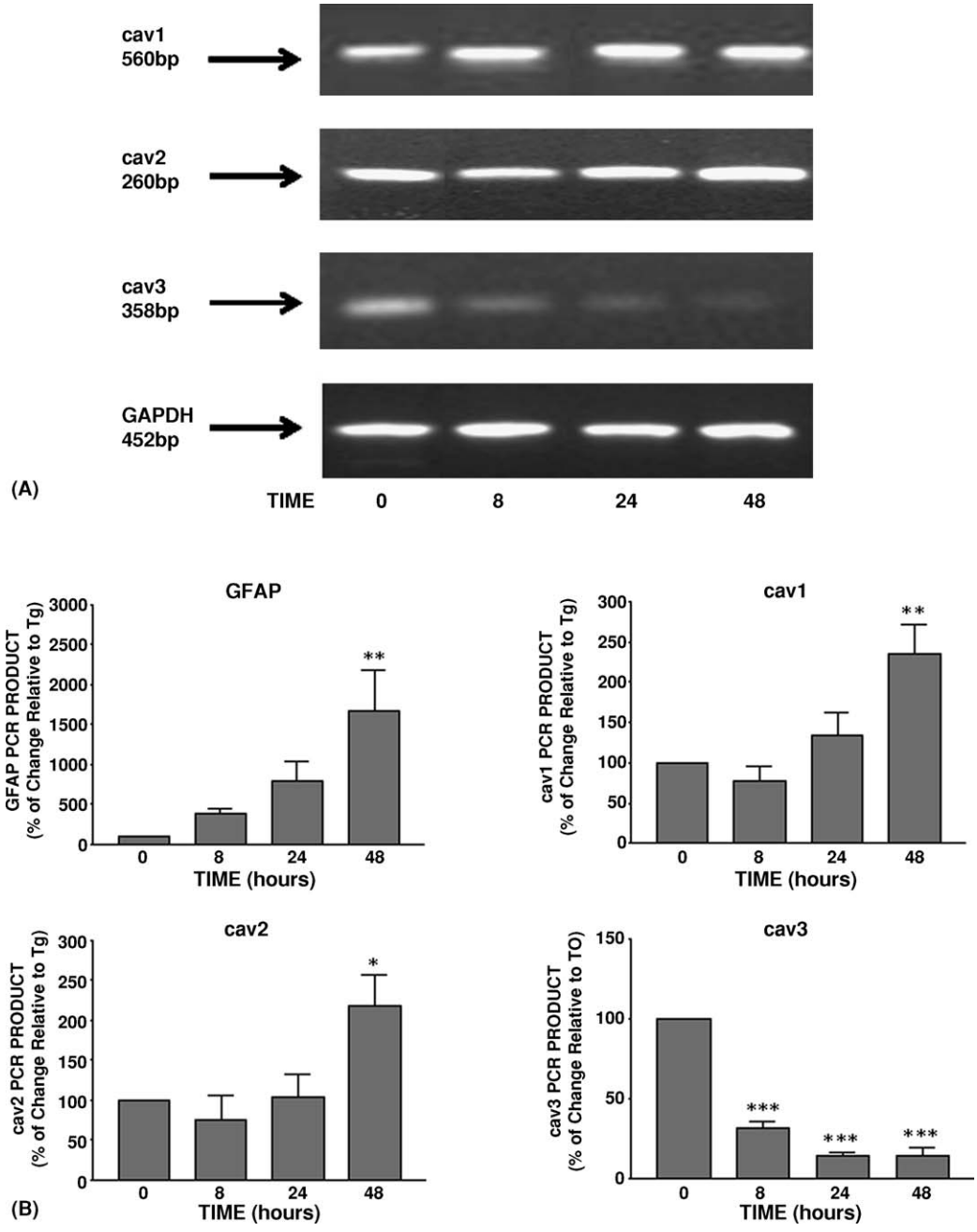

Fig. 4. Conventional (panel A) and real-time (panel B) RT-PCR analysis of caveolin isoform mRNA expression during db-cAMP-induced differentiation of C6 glioma cells. (Panel A) RT-PCR was performed using total RNA derived from 1 mM db-cAMP treated and untreated C6 glioma cells. mRNA expression of the different caveolin isoforms was determined at different time points (T_0, T_8, T_{24}, and T_{48}) after induction of differentiation. Specific primers for the amplification of cav1, cav2, cav3, and GAPDH were used (see Section 2). Reaction products were separated using a 2% agarose gel containing ethidium bromide. The expected sizes of the reaction products are marked on the left side of the figure. Time (h) is indicated horizontally. (Panel B) Real-time RT-PCR analysis was performed to determine quantitative changes in caveolin expression during db-cAMP-induced differentiation of C6 astroglioma cells. The astrocyte marker GFAP was used as control for differentiation of C6 glioma cells into an astrocyte-like morphology. Data represents values normalized against GAPDH and expressed as % of change relative to the control (T_0). Each bar represents the mean ± S.E.M. of at least four independent experiments (cav1: $n = 5$; cav2: $n = 5$; cav3: $n = 4$; GFAP: $n = 5$) ($^{*}p \leq 0.05$; $^{**}p \leq 0.01$; $^{***}p \leq 0.001$).

3.6. Indirect immunofluorescence analysis of cav3 in differentiated C6 glioma cells

The findings on the subcellular distribution of cav1 and cav2 immunoreactivity in C6 glioma cells of a previous study (Silva et al., 1999), and those reported here for the three isoforms (Fig. 3), have been obtained with mid-passage C6 glioma cells, not induced to differentiate into an astrocyte-like phenotype. Therefore, lase-scanning confocal microscopy was undertaken to address the latter issue and,

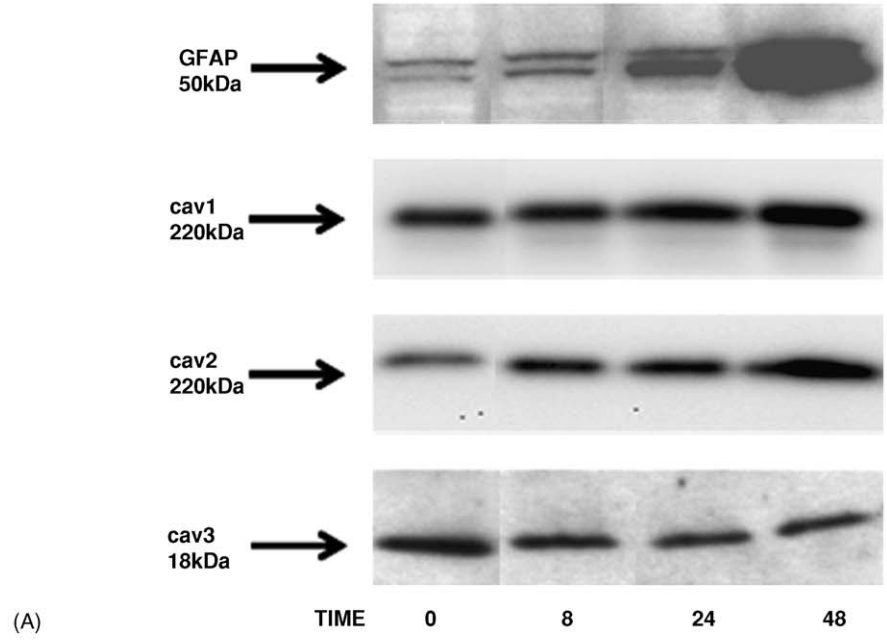

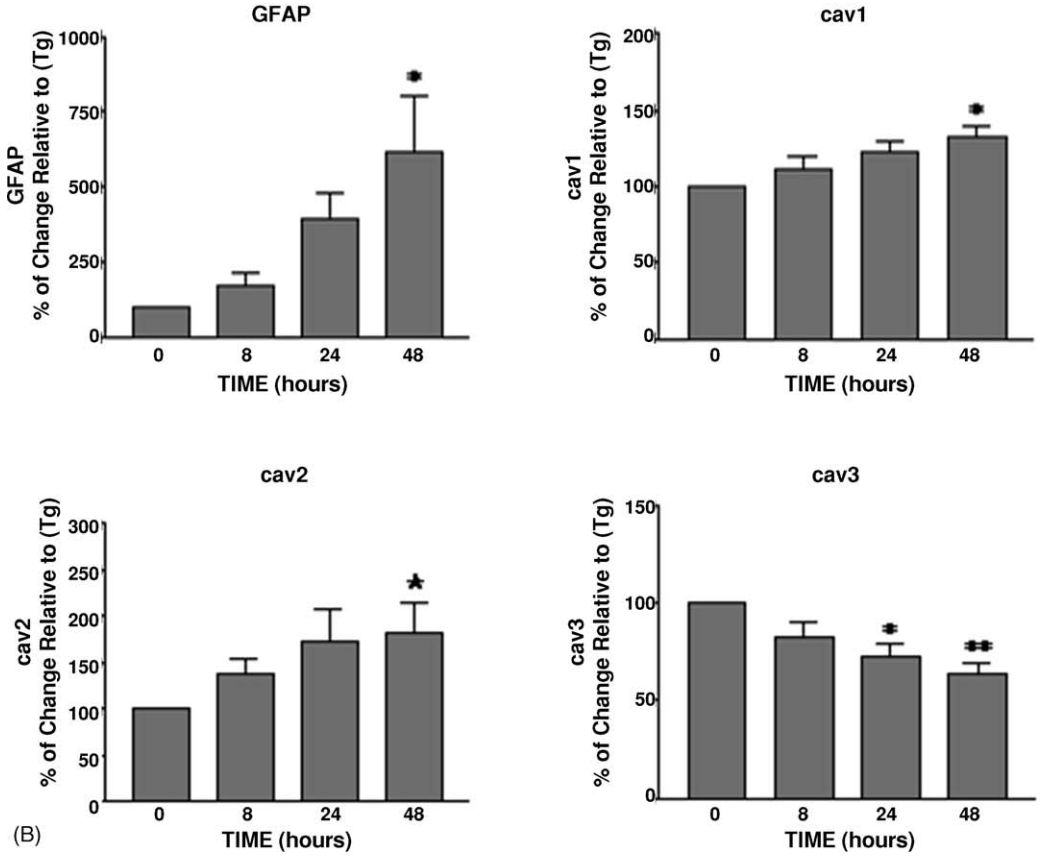

Fig. 5. Analysis of caveolin isoform and GFAP protein expression during db-cAMP-induced differentiation of C6 glioma cells. (Panel A) Immunoblot analysis of the expression of the different caveolin isoforms and GFAP using total homogenate fractions from C6 glioma cells obtained before (T_0) and at different time (h) points after treatment with 1 mM db-cAMP (T_8, T_{24}, and T_{48}). Equal amounts (~10 μg) of sample protein were loaded and then separated by SDS-PAGE. The relative protein content was verified by means of India ink staining. Representative gels are shown at the top of each graph. The astrocyte marker GFAP was used as control for differentiation of glioma cells to an astrocyte-like morphology. (Panel B) Densitometric analysis of caveolin and GFAP immunoblots. Optical density analysis of the specific bands was performed and corrected by protein content. Results represent the % of change relative to the control (T_0). Each bar represents the mean ± S.E.M. of at least four independent experiments (cav1: $n = 6$; cav2: $n = 6$; cav3: $n = 5$; GFAP: $n = 4$) ($^{*}p \leq 0.05$; $^{**}p \leq 0.01$; $^{***}p \leq 0.001$).

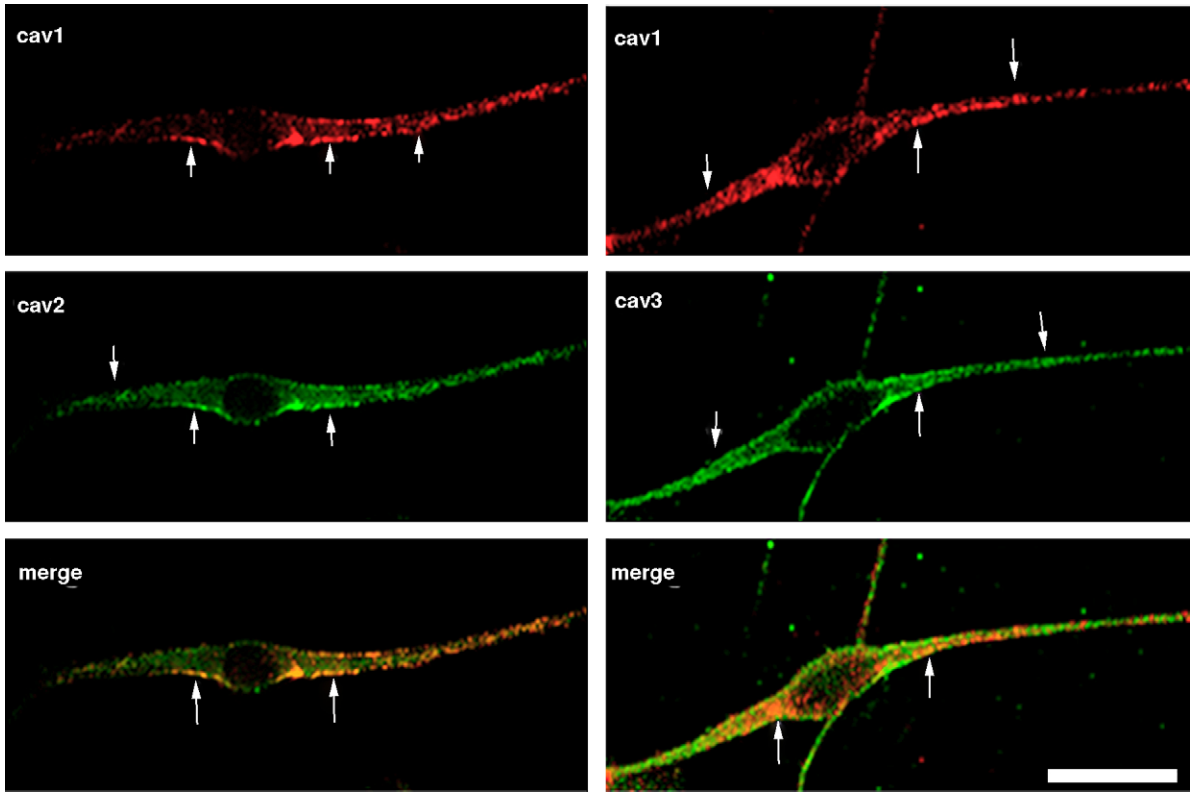

Fig. 6. Analysis of the expression and co-localization of the caveolin isoforms in differentiated C6 glioma cells using laser-scanning confocal microscopy. The top row images correspond to immunolabeling using a cav1 primary antibody and an Alexa 633-coupled secondary antibody (red). The middle row images correspond to immunolabeling of cav2 (left) or cav3 (right) with Alexa 488-coupled secondary antibodies (green). The bottom row images correspond to the merge of the cav1/cav2 and cav1/cav3 immunofluorescence signals to determine their co-localization in ''astrocyte-like'' differentiated C6 glioma cells. The three isoforms display patterns of subcellular distribution typical of caveolins, characterized by intensely fluorescent puncta throughout the cytoplasm (arrow heads) and plasmalemma caveolar micropatches (arrow). Perinuclear staining was also detected, consistent with caveolin's localization in the Golgi. On the merged images (bottom row), co-localization of cav1/cav2 and cav1/cav3 is indicated by the yellow fluorescence signal (arrows). Scale bar: 10 μm. ''For interpretation of the references to color in this figure legend, the reader is referred to the web version of the article.''

most importantly, to determine if changes in caveolin mRNA and protein expression are accompanied by spatial alterations in the subcellular distribution of the caveolin isoform in differentiated C6 glioma cells. In differentiated C6 glioma cells, cav1 and cav2 also display patterns of subcellular distribution characterized by intensely fluorescent puncta throughout the cytoplasm and diffuse micropatches at the level of the plasmalemma and perinuclear staining (Fig. 6). Fig. 6 also demonstrates co-localization of both cav1 and cav2 in plasmalemmal caveolar micropatches. Caveolin-3 message and protein levels can still be detected in C6 glioma cells despite the decline in their relative expression in differentiated C6 glioma cells (Figs. 4 and 5). A similar subcellular distribution pattern was revealed for cav3 in differentiated C6 glioma cells, as revealed by its expression in plasmalemmal caveolar micropatches, puncta and perinuclear staining. Co-localization of cav1 and cav3 in plasmalemmal caveolar micropatches was also observed (Fig. 6), resembling the co-localization pattern of cav1/cav2.

4. Discussion

The first evidence on the expression of caveolins (cav1 and cav2) and CAV in a glial tumor cell line was obtained in studies conducted on rat C6 astroglioma cells (Silva et al., 1999). The presence of cav1 in C6 cells was corroborated, and further expanded to the rat astroglial cell line DI TNC(1), as well as several cell lines derived from human glioblastoma tumors (Cameron et al., 2002). The present study extends the characterization of the caveolin gene family in C6 astroglia to cav3, and assesses the expression of the three caveolins during the experimentally induced differentiation of C6 cells. As a first approach, the expression of the mRNA for the three known caveolin isoforms was detected in C6 cells expressing an oligodendrocyte-like phenotype cells via RT-PCR analysis (conventional and real-time). These findings substantiate the expression of the message for the cav1 isoform in C6 cells, while providing evidence for the first time of the expression of the mRNA for the cav2 and cav3 isoforms in this cell line.

The detection of the cav3 isoform is of particular importance since it is usually regarded as a muscle-specific isoform. Therefore, to unequivocally demonstrate the expression of cav3 in C6 cells, its presence was further confirmed by immunoblot analysis of total cell homogenates, density gradient sedimentation, and indirect immunofluorescence. The analysis revealed a cav3 immunoreactivity of ~18 kDa, with buoyant density and detergent-insolubility properties typical of the caveolins. The expression of cav3 is especially noteworthy, since it has been detected in oligodendrocytes and astrocytes (Ikezu et al., 1998), and has been claimed to have special relevance to the pathophysiology of Alzheimer's disease (AD) (Nishiyama et al., 1999). Similarly, cav1 protein levels in the hippocampus and caveolin mRNA in the frontal cortex have been shown to be up-regulated in AD patients by approximately two-fold (Gaudreault et al., 2004).

The findings presented in this study are consistent with those conducted on primary cell cultures and established glial cell lines, which demonstrated the expression of the cav1 and cav2 isoforms (Bushby, 1999; Cameron et al., 2002; Colasanti et al., 1998; Mikol et al., 1999; Silva et al., 1999). Additional studies on brain tissue have also confirmed expression of the three caveolin isoforms, including apparent higher molecular weight species, probably due to their oligomerization and protein-interaction properties (Ikezu et al., 1998). Taking advantage of laser-scanning confocal microscopy, the co-localization of the three caveolin isoforms was evaluated in C6 cells, as well. As it has been previously established, cav1 and cav2 display patterns of subcellular distribution characterized by intensely fluorescent puncta throughout the cytoplasm and diffuse micropatches at the level of the plasmalemma, consistent with CAV, with significant co-localization of both isoforms. Perinuclear staining was also detected, consistent and suggestive of caveolin's localization in C6 glioma cells in the *trans* Golgi region. The subcellular distribution patterns of cav1 and cav2 were similar in undifferentiated C6 cells, and the experimentally induced astrocyte-like phenotype. A similar subcellular distribution and co-localization pattern was also revealed for cav3 and cav1. The findings on caveolin immunoreactive species in both C6 cell phenotypes and the LSCM results correlate with the presence of morphologically identifiable CAV (Silva et al., 1999).

Studies on the regulation of caveolin expression in glial cells have been very limited to date and restricted to cav1 and cav2 (Zschoecke et al., 2005). The results presented here, provide additional evidence on the regulation of cav1 and cav2, and the first results on the regulation of cav3 expression during differentiation of a cultured glial cell line. The present study demonstrates an up-regulation of cav1 and cav2, accompanied by a prominent down-regulation of the cav3 isoform, during the experimentally induced differentiation of C6 into an astrocyte-like phenotype. These patterns were seen for both the mRNA and protein, although to a lesser degree with the cav2 protein (*t*-test analysis also revealed a significant increase during differentiation after 48 h). These findings contrast those of the recent study by Zschoecke et al. (2005), where down-regulation of cav1 and cav2 is observed during forskolin- and TGFα-induced differentiation of primary cell cultures of astrocytes derived from brain cortex and striatum. Most importantly, this down-regulation was seen in cortical and striatal astrocytes, but not in those from cerebellum and midbrain. Therefore, relative regulation of caveolin isoform expression is dependent on the brain region from which glial cells are derived. Regulation of caveolin expression may also vary depending on the glial cell line utilized, or the use of primary cell cultures.

It has been previously shown that cyclic AMP via protein kinase A activation down-regulates cav1 mRNA and protein expression in CHO cells (Engelman et al., 1999) and rat cardiac myoblasts (H9C2 cells) (Yamamoto et al., 1999). In contrast, forskolin and IBMX were shown to induce a biphasic change in cav1 mRNA expression in rat aortic smooth muscle cells (RASMC), with an initial increase followed by a decrease (Yamamoto et al., 1999). In the latter study, the levels of cav1 and cav3 proteins were also decreased by forskolin treatment, but only after 60–72 h in RASMC and 24–36 h in H9C2 cells. In contrast, the expression of cav2 remained similar in both cells and decreased to a small degree after prolonged treatment. These findings demonstrate that expression of caveolin is down-regulated by cAMP signal in a caveolin subtype and cell type dependent manner. This concept is supported by the results presented here in C6 cells where differential patterns of caveolin mRNA and protein expression are observed during db-cAMP-induced differentiation of these cells. In the case of cultured glia, differences in patterns of regulation may relate to differentiation conditions, such as the agents used (db-cAMP versus forskolin), and relative serum concentrations (low serum (1%) conditions in C6 cells studies). Indeed, the work of Ikezu et al. (1998) demonstrates that culture conditions differentially affect the expression of the three caveolin isoforms. The study suggests that conditions used to grow astroglial cells promote expression of cav1 and cav2, and down-regulate the expression of cav3 (Ikezu et al., 1998). In the case of astrocytes, in vivo studies demonstrated that astrocytes preferentially express caveolin-3 while in culture, they express cav1 and cav2 (Ikezu et al., 1998). In other cell systems, increase in the total content of cav1 has been reported in NG108–15 cells treated and induced to differentiate with PGE_1 and theophylline (Toselli et al., 2001). While studies on cav1 and cav2 in PC12 cells and dorsal root ganglion (DRG) neurons showed that cav1 expression is up-regulated on day 4 after nerve growth factor (NGF) treatment, whereas cav2 is transiently up-regulated early in the differentiation program (reaching its maximal at day 3), and rapidly down-regulated at day 4 after NGF treatment. Interestingly, cav2 is also up-regulated in response to the mechanical injury of differentiated PC12

cells, an event strictly dependent on continued treatment with NGF (Galbiati et al., 1998). According to Galbiati et al. (1998), induction of cav1 and cav2 during NGF-induced differentiation is consistent with the idea that caveolins are generally induced during differentiation processes and their expression is highest in terminally differentiated non-dividing cells (Galbiati et al., 1998). Studies on the differentiation of C2C12 cells from myoblasts to myotubes (which lead to a dramatic up-regulation of cav3 with no changes in cav2 expression), also support the notion that caveolins can be independently up-regulated or down-regulated in response to a variety of distinct cellular cues (Scherer et al., 1997).

The prominent down-regulation of cav3 (protein and mRNA) seen during differentiation of C6 cells into an astrocyte-like phenotype, suggests regulation of cav3 expression at the transcriptional level. Down-regulation of the cav3 isoform has also been seen during chick brain development at embryonic day 4 in the myotome and neural tube; meanwhile, brain immunolabeling is present at embryonic day 6 and its intensity reduced at embryonic day 8 (Shin et al., 2003). The down-regulation seen for cav3 in C6 astroglia is of utmost significance, since further analysis of this experimentally induced down-regulation of cav3 in C6 may shed light on potential neuro- or glio-protective mechanisms in Alzheimer's disease. The thorough understanding of the mechanisms inducing down-regulation of cav3, will present means to counteract the dramatic up-regulation of cav3 immunoreactivity seen in astroglial cells surrounding senile plaques (Nishiyama et al., 1999) in brain tissue sections from authentic AD patients and an established transgenic mouse model of AD. In the latter study, cav3 was shown to physically interact and co-localize with the amyloid precursor protein (APP) both in vivo and in vitro. Immunoreactivities of APP and presenilins were concomitantly increased in cav3-positive astrocytes. Because the presenilins also form a physical complex with cav3, CAV may provide a common platform for APP and the presenilins to associate in astrocytes. In AD, augmented expression of cav3 and presenilins in reactive astrocytes may alter APP processing, leading to the overproduction of its toxic amyloid metabolites (Nishiyama et al., 1999). The latter pathophysiological process may be altered by agents targeted to disrupt the CAV platform, or by targeted down-regulation of cav3.

Early morphological studies identified plasmalemmal vesicles in peripheral Schwann cells (Mugnaini et al., 1977), fibrous astrocytes from cat optic nerve (Massa, 1982), and mixed cultures of rat fetal glial cells (Massa and Mugnaini, 1985). The caveolins in glia are linked to an active subcellular transport machinery, like a developed endocytic system mainly composed of caveolae, clathrin-coated pits and vesicles, tubulo-vesicular and spheric endosomes, multivesicular bodies, and lysosomes (Silva et al., 1999; Megias et al., 2000). Furthermore, the glial CAV compartment has been proposed to play an important role in the regulation of drug transport in the nervous system (Demeule et al., 2000; Ronaldson et al., 2004), signal transduction (Abulrob et al., 2004; Arvanitis et al., 2004; Colasanti et al., 1998; Ge and Pachter, 2004; Mentlein et al., 2001; Teixeira et al., 1999), and cholesterol homeostasis (Ito et al., 2002, 2004). The present study furthers the value of the C6 astroglial cells model system for the assessment of the role of CAV and caveolins in glial cell maturation, differentiation, and signal transduction. The recent identification of CAV and caveolins in the brain and in glial cells poses itself as fertile ground for the discovery of potentially novel emerging functions of this group of scaffolding molecules.

Acknowledgments

This work was supported in part by NIH SCORE Grants S06-GM08224 and S06-GM50695 awarded to WIS and HMM, respectively. MRD is a recipient of a Minority Supplemental Postdoctoral Award under Grant S06-GM08224. Graduate student GV and undergraduate student JJ were supported by the NIH-MBRS-RISE Grant GM61838.

References

Abulrob, A., Giuseppin, S., Andrade, M.F., McDermid, A., Moreno, M., Stanimirovic, D., 2004. Interactions of EGFR and caveolin-1 in human glioblastoma cells: evidence that tyrosine phosphorylation regulates EGFR association with caveolae. Oncogene 23 (41), 6967–6979.

Arvanitis, D.N., Wang, H., Bagshaw, R.D., Callahan, J.W., Boggs, J.M., 2004. Membrane-associated estrogen receptor and caveolin-1 are present in central nervous system myelin and oligodendrocyte plasma membranes. J. Neurosci. Res. 75 (5), 603–613.

Benda, P., Lightbody, J., Sato, G., Levine, L., Sweet, W., 1968. Differentiated rat glial cell strain in tissue culture. Science 161 (839), 370–371.

Bruns, R.R., Palade, G.E., 1968a. Studies on blood capillaries. Part I: general organization of blood capillaries in muscle. J. Cell Biol. 37 (2), 244–276.

Bruns, R.R., Palade, G.E., 1968b. Studies on blood capillaries. Part II: transport of ferritin molecules across the wall of muscle capillaries. J. Cell Biol. 37 (2), 277–299.

Bushby, K.M., 1999. The limb-girdle muscular dystrophies-multiple genes, multiple mechanisms. Hum. Mol. Genet. 8 (10), 1875–1882.

Cameron, P.L., Ruffin, J.W., Bollag, R., Rasmussen, H., Cameron, R.S., 1997. Identification of caveolin and caveolin-related proteins in the brain. J. Neurosci. 17 (24), 9520–9535.

Cameron, P.L., Liu, C., Smart, D.K., Hantus, S.T., Fick, J.R., Cameron, R.S., 2002. Caveolin-1 expression is maintained in rat and human astroglioma cell lines. Glia 37 (3), 275–290.

Chini, B., Parenti, M., 2004. G-protein coupled receptors in lipid rafts and caveolae: how, when and why do they go there? J. Mol. Endocrinol. 32 (2), 325–338.

Cohen, A.W., Combs, T.P., Scherer, P.E., Lisanti, M.P., 2003. Role of caveolin and caveolae in insulin signaling and diabetes. Am. J. Physiol. Endocrinol. Metab. 285 (6), E1151–E1160.

Cohen, A.W., Hnasko, R., Schubert, W., Lisanti, M.P., 2004. Role of caveolae and caveolins in health and disease. Physiol. Rev. 84 (4), 1341–1379.

Colasanti, M., Persichini, T., Fabrizi, C., Cavalieri, E., Venturini, G., Ascenzi, P., Lauro, G.M., Suzuki, H., 1998. Expression of a NOS-III-like protein in human astroglial cell culture. Biochem. Biophys. Res. Commun. 252 (3), 552–555.

Conner, S.D., Schmid, S.L., 2003. Regulated portals of entry into the cell. Nature 422 (6927), 37–44.

Demeule, M., Jodoin, J., Gingras, D., Beliveau, R., 2000. *P*-glycoprotein is localized in caveolae in resistant cells and in brain capillaries. FEBS Lett. 466 (2–3), 219–224.

Engelman, J.A., Zhang, X., Galbiati, F., Volonte, D., Sotgia, F., Pestell, R.G., Minetti, C., Scherer, P.E., Okamoto, T., Lisanti, M.P., 1998. Molecular genetics of the caveolin gene family: implications for human cancers, diabetes, Alzheimer disease, and muscular dystrophy. Am. J. Hum. Genet. 63 (6), 1578–1587.

Engelman, J.A., Zhang, X.L., Razani, B., Pestell, R.G., Lisanti, M.P., 1999. p42/44 MAP kinase-dependent and -independent signaling pathways regulate caveolin-1 gene expression: activation of Ras-MAP kinase and protein kinase a signaling cascades transcriptionally down-regulates caveolin-1 promoter activity. J. Biol. Chem. 274 (45), 32333–32341.

Everson, W.V., Smart, E.J., 2001. Influence of caveolin, cholesterol, and lipoproteins on nitric oxide synthase: implications for vascular disease. Trends Cardiovasc. Med. 11 (6), 246–250.

Frank, P.G., Woodman, S.E., Park, D.S., Lisanti, M.P., 2003. Caveolin, caveolae, and endothelial cell function. Arterioscler. Thromb. Vasc. Biol. 23 (7), 1161–1168.

Galbiati, F., Volonte, D., Gil, O., Zanazzi, G., Salzer, J.L., Sargiacomo, M., Scherer, P.E., Engelman, J.A., Schlegel, A., Parenti, M., et al., 1998. Expression of caveolin-1 and -2 in differentiating PC12 cells and dorsal root ganglion neurons: caveolin-2 is up-regulated in response to cell injury. Proc. Natl. Acad. Sci. U.S.A. 95 (17), 10257–10262.

Galbiati, F., Razani, B., Lisanti, M.P., 2001. Caveolae and caveolin-3 in muscular dystrophy. Trends Mol. Med. 7 (10), 435–441.

Gaudreault, S.B., Dea, D., Poirier, J., 2004. Increased caveolin-1 expression in Alzheimer's disease brain. Neurobiol. Aging 25 (6), 753–759.

Ge, S., Pachter, J.S., 2004. Caveolin-1 knockdown by small interfering RNA suppresses responses to the chemokine monocyte chemoattractant protein-1 by human astrocytes. J. Biol. Chem. 279 (8), 6688–6695.

Glenney Jr., J.R., 1992. The sequence of human caveolin reveals identity with VIP21, a component of transport vesicles. FEBS Lett. 314 (1), 45–48.

Glenney Jr., J.R., Soppet, D., 1992. Sequence and expression of caveolin: a protein component of caveolae plasma membrane domains phosphorylated on tyrosine in *Rous sarcoma* virus-transformed fibroblasts. Proc. Natl. Acad. Sci. U.S.A. 89 (21), 10517–10521.

Hashimoto, M., Masliah, E., 2003. Cycles of aberrant synaptic sprouting and neurodegeneration in Alzheimer's and dementia with Lewy bodies. Neurochem. Res. 28 (11), 1743–1756.

Helms, J.B., Zurzolo, C., 2004. Lipids as targeting signals: lipid rafts and intracellular trafficking. Traffic 5 (4), 247–254.

Henke, R.C., Hancox, K.A., Jeffrey, P.L., 1996. Characterization of two distinct populations of detergent resistant membrane complexes isolated from chick brain tissues. J. Neurosci. Res. 45 (5), 617–630.

Hnasko, R., Lisanti, M.P., 2003. The biology of caveolae: lessons from caveolin knockout mice and implications for human disease. Mol. Interv. 3 (8), 445–464.

Ikezu, T., Ueda, H., Trapp, B.D., Nishiyama, K., Sha, J.F., Volonte, D., Galbiati, F., Byrd, A.L., Bassell, G., Serizawa, H., et al., 1998. Affinity-purification and characterization of caveolins from the brain: differential expression of caveolin-1, -2, and -3 in brain endothelial and astroglial cell types. Brain Res. 804 (2), 177–192.

Ito, J., Nagayasu, Y., Kato, K., Sato, R., Yokoyama, S., 2002. Apolipoprotein A-I induces translocation of cholesterol, phospholipid, and caveolin-1 to cytosol in rat astrocytes. J. Biol. Chem. 277 (10), 7929–7935.

Ito, J.I., Li, H., Nagayasu, Y., Kheirollah, A., Yokoyama, S., 2004. Apolipoprotein A-I induces translocation of protein kinase-Calpha to a cytosolic lipid–protein particle in astrocytes. J. Lipid Res.

Koleske, A.J., Baltimore, D., Lisanti, M.P., 1995. Reduction of caveolin and caveolae in oncogenically transformed cells. Proc. Natl. Acad. Sci. U.S.A. 92 (5), 1381–1385.

Lakadamyali, M., Rust, M.J., Zhuang, X., 2004. Endocytosis of influenza viruses. Microb. Infect. 6 (10), 929–936.

Lisanti, M.P., Tang, Z., Scherer, P.E., Kubler, E., Koleske, A.J., Sargiacomo, M., 1995a. Caveolae, transmembrane signalling and cellular transformation. Mol. Membr. Biol. 12 (1), 121–124.

Lisanti, M.P., Tang, Z., Scherer, P.E., Sargiacomo, M., 1995b. Caveolae purification and glycosylphosphatidylinositol-linked protein sorting in polarized epithelia. Methods Enzymol. 250, 655–668.

Livak, K.J., Schmittgen, T.D., 2001. Analysis of relative gene expression data using real-time quantitative PCR and the 2(−delta delta C(T)) method. Methods 25 (4), 402–408.

Massa, P.T., 1982. Plasmalemmal vesicles (caveolae) of fibrous astrocytes of the cat optic nerve. Am. J. Anat. 165 (1), 69–81.

Massa, P.T., Mugnaini, E., 1985. Cell–cell junctional interactions and characteristic plasma membrane features of cultured rat glial cells. Neuroscience 14 (2), 695–709.

Megias, L., Guerri, C., Fornas, E., Azorin, I., Bendala, E., Sancho-Tello, M., Duran, J.M., Tomas, M., Gomez-Lechon, M.J., Renau-Piqueras, J., 2000. Endocytosis and transcytosis in growing astrocytes in primary culture: possible implications in neural development. Int. J. Dev. Biol. 44 (2), 209–221.

Mentlein, R., Held-Feindt, J., Krisch, B., 2001. Topology of the signal transduction of the G protein-coupled somatostatin receptor sst2 in human glioma cells. Cell Tissue Res. 303 (1), 27–34.

Mikol, D.D., Hong, H.L., Cheng, H.L., Feldman, E.L., 1999. Caveolin-1 expression in Schwann cells. Glia 27 (1), 39–52.

Mineo, C., Anderson, R.G., 2001. Potocytosis: Robert Feulgen lecture. Histochem. Cell Biol. 116 (2), 109–118.

Mugnaini, E., Osen, K.K., Schnapp, B., Friedrich Jr., V.L., 1977. Distribution of Schwann cell cytoplasm and plasmalemmal vesicles (caveolae) in peripheral myelin sheaths: an electron microscopic study with thin sections and freeze-fracturing. J. Neurocytol. 6 (6), 647–668.

Nichols, B., 2003. Caveosomes and endocytosis of lipid rafts. J. Cell Sci. 116 (Pt. 23), 4707–4714.

Nishino, I., Ozawa, E., 2002. Muscular dystrophies. Curr. Opin. Neurol. 15 (5), 539–544.

Nishiyama, K., Trapp, B.D., Ikezu, T., Ransohoff, R.M., Tomita, T., Iwatsubo, T., Kanazawa, I., Hsiao, K.K., Lisanti, M.P., Okamoto, T., 1999. Caveolin-3 upregulation activates beta-secretase-mediated cleavage of the amyloid precursor protein in Alzheimer's disease. J. Neurosci. 19 (15), 6538–6548.

Okamoto, T., Schlegel, A., Scherer, P.E., Lisanti, M.P., 1998. Caveolins, a family of scaffolding proteins for organizing "preassembled signaling complexes" at the plasma membrane. J. Biol. Chem. 273 (10), 5419–5422.

Palade, G.E., 1961. Blood capillaries of the heart and other organs. Circulation 24, 368–388.

Pfeiffer, S.E., Herschman, H.R., Lightbody, J., Sato, G., 1970. Synthesis by a clonal line of rat glial cells of a protein unique to the nervous system. J. Cell Physiol. 75 (3), 329–339.

Pietiainen, V., Marjomaki, V., Upla, P., Pelkmans, L., Helenius, A., Hyypia, T., 2004. Echovirus 1 endocytosis into caveosomes requires lipid rafts, dynamin II, and signaling events. Mol. Biol. Cell 15 (11), 4911–4925.

Quest, A.F., Leyton, L., Parraga, M., 2004. Caveolins, caveolae, and lipid rafts in cellular transport, signaling, and disease. Biochem. Cell. Biol. 82 (1), 129–144.

Razani, B., Lisanti, M.P., 2001. Caveolin-deficient mice: insights into caveolar function human disease. J. Clin. Invest. 108 (11), 1553–1561.

Razani, B., Schlegel, A., Lisanti, M.P., 2000. Caveolin proteins in signaling, oncogenic transformation and muscular dystrophy. J. Cell. Sci. 113 (Pt. 12), 2103–2109.

Razani, B., Schlegel, A., Liu, J., Lisanti, M.P., 2001. Caveolin-1, a putative tumour suppressor gene. Biochem. Soc. Trans. 29 (Pt. 4), 494–499.

Rohde, M., Muller, E., Chhatwal, G.S., Talay, S.R., 2003. Host cell caveolae act as an entry-port for group A streptococci. Cell Microbiol. 5 (5), 323–342.

Ronaldson, P.T., Bendayan, M., Gingras, D., Piquette-Miller, M., Bendayan, R., 2004. Cellular localization and functional expression of *P*-glycoprotein in rat astrocyte cultures. J. Neurochem. 89 (3), 788–800.

Rothberg, K.G., Heuser, J.E., Donzell, W.C., Ying, Y.S., Glenney, J.R., Anderson, R.G., 1992. Caveolin, a protein component of caveolae membrane coats. Cell 68 (4), 673–682.

Sargiacomo, M., Sudol, M., Tang, Z., Lisanti, M.P., 1993. Signal transducing molecules and glycosyl-phosphatidylinositol-linked proteins form a caveolin-rich insoluble complex in MDCK cells. J. Cell Biol. 122 (4), 789–807.

Scherer, P.E., Lewis, R.Y., Volonte, D., Engelman, J.A., Galbiati, F., Couet, J., Kohtz, D.S., van Donselaar, E., Peters, P., Lisanti, M.P., 1997. Cell-type and tissue-specific expression of caveolin-2: caveolins 1 and 2 colocalize and form a stable hetero-oligomeric complex in vivo. J. Biol. Chem. 272 (46), 29337–29346.

Shatz, M., Liscovitch, M., 2004. Caveolin-1 and cancer multidrug resistance: coordinate regulation of pro-survival proteins? Leuk. Res. 28 (9), 907–908.

Shin, D.H., Kim, J.S., Kwon, B.S., Lee, K.S., Kim, J.W., Kim, M.H., Cho, S.S., Lee, W.J., 2003. Caveolin-3 expression during early chicken development. Brain Res. Dev. Brain Res. 141 (1–2), 83–89.

Silva, W.I., Maldonado, H.M., Lisanti, M.P., Devellis, J., Chompre, G., Mayol, N., Ortiz, M., Velazquez, G., Maldonado, A., Montalvo, J., 1999. Identification of caveolae and caveolin in C6 glioma cells. Int. J. Dev. Neurosci. 17 (7), 705–714.

Simons, K., Toomre, D., 2000. Lipid rafts and signal transduction. Nat. Rev. Mol. Cell Biol. 1 (1), 31–39.

Teixeira, A., Chaverot, N., Schroder, C., Strosberg, A.D., Couraud, P.O., Cazaubon, S., 1999. Requirement of caveolae microdomains in extracellular signal-regulated kinase and focal adhesion kinase activation induced by endothelin-1 in primary astrocytes. J. Neurochem. 72 (1), 120–128.

Toselli, M., Taglietti, V., Parente, V., Flati, S., Pavan, A., Guzzi, F., Parenti, M., 2001. Attenuation of G protein-mediated inhibition of N-type calcium currents by expression of caveolins in mammalian NG108–15 cells. J. Physiol. 536 (Pt. 2), 361–373.

Williams, T.M., Lisanti, M.P., 2004. The caveolin proteins. Genome Biol. 5 (3), 214.

Woodman, S.E., Sotgia, F., Galbiati, F., Minetti, C., Lisanti, M.P., 2004. Caveolinopathies: mutations in caveolin-3 cause four distinct autosomal dominant muscle diseases. Neurology 62 (4), 538–543.

Yamamoto, M., Okumura, S., Oka, N., Schwencke, C., Ishikawa, Y., 1999. Downregulation of caveolin expression by cAMP signal. Life Sci. 64 (15), 1349–1357.

Zschoecke, J., Bayatti, N., Behl, C., 2005. Caveolin and GLT-1 gene expression is reciprocally regulated in primary astrocytes: association of GLT-1 with non-caveolar lipid rafts. Glia 49 (2), 275–287.